

Artificial gravity field

Larry C. Markley, John F. Lindner*

Physics Department, The College of Wooster, Wooster, OH 44691, United States



ARTICLE INFO

Article history:

Received 8 December 2012

Accepted 12 January 2013

Available online 9 February 2013

Keywords:

Gravity

General relativity

Stress-energy

ABSTRACT

Using computer algebra to run Einstein's equations "backward", from field to source rather than from source to field, we design an artificial gravity field for a space station or spaceship. Everywhere inside astronauts experience normal Earth gravity, while outside they float freely. The stress-energy that generates the field contains exotic matter of negative energy density but also relies importantly on pressures and shears, which we describe. The same techniques can be readily used to design other interesting spacetimes and thereby elucidate the connection between the source and field in general relativity.

© 2013 The Authors. Published by Elsevier B.V. Open access under CC BY-NC-ND license.

1. Introduction

The Einstein field equations of general relativity are nonlinear partial differential equations for spacetime curvature given a source of stress, energy, and momentum. They are notoriously difficult to solve exactly. However, two strategies radically simplify the problem. First, one can reverse the equations, so that instead of integrating to find the curvature given the stress-energy, one differentiates the curvature of a given spacetime to find the stress-energy needed to create it. Second, one can exploit the wide availability of powerful computer algebra software. These strategies tame a wide range of interesting problems.

As an example, we design an artificial gravity field for a cylindrical space station or spaceship. Specifically, we stipulate that inside a cylinder the spacetime curvature (and hence the gravity) will be the same as near Earth, but outside the cylinder spacetime will be flat (like empty space far from any stars). We join the two spacetimes smoothly and continuously across a finite thickness (of the spaceship's hull). Everywhere inside our astronauts experience normal Earth surface gravity, but outside they float freely. We highlight the important role of pressures, tensions, and shears – as well as energy – in creating this spacetime. Such speculative spacetime engineering provides an illuminating approach to understanding general relativity.

Section 2 makes the paper self-contained and fixes its notation and conventions. For nonspecialists, it reviews the minimum general relativity needed to create and test the artificial gravity field,

including the field equations and the geodesic equations of motion, but with special attention to the structure of the stress-energy source tensor. Section 3 fashions the desired spacetime metric and differentiates it to obtain the needed stress-energy. It tests the field by numerically releasing test particles inside and outside the spaceship. It compares the field with that of a Newtonian slab and briefly discusses the feasibility of marshaling the stress-energy needed to create the field. Section 4 suggests future projects and extensions, including possible experiments. A supplementary *Mathematica* notebook [1] provides the details for all the analytics and numerics in the paper and may be readily modified to further explore Einsteinian gravity.

2. General relativity primer

This section follows John Archibald Wheeler's famous summary of general relativity: matter tells spacetime how to curve, and spacetime tells matter how to move [2,3]. For simplicity, it uses natural Planck units where $G = c = 1$.

2.1. Curvature

Locate an event in spacetime with the rectangular coordinates

$$x^\mu \leftrightarrow \begin{bmatrix} x^0 \\ x^1 \\ x^2 \\ x^3 \end{bmatrix} = \begin{bmatrix} t \\ x \\ y \\ z \end{bmatrix}, \quad (1)$$

where $x^0 = t$ is time, $\{x, y, z\}$ is a place in space, and the superscripts are indices not exponents. Determine invariant interval $d\sigma$ between neighboring events in spacetime by the line element

* Corresponding author. Tel.: +1 330 263 2120; fax: +1 330 263 2516.

E-mail address: jlindner@wooster.edu (J.F. Lindner).

$$d\sigma^2 = \sum_{\mu=0}^3 \sum_{\nu=0}^3 g_{\mu\nu} dx^\mu dx^\nu = g_{\mu\nu} dx^\mu dx^\nu, \quad (2)$$

where $g_{\mu\nu} = g_{\nu\mu}$ is the metric, and there is an implied sum over repeated upper and lower indices. In flat spacetime far from any stress or energy, the Minkowski metric

$$g_{\mu\nu}^M = \eta_{\mu\nu} \leftrightarrow \begin{bmatrix} -1 & 0 & 0 & 0 \\ 0 & +1 & 0 & 0 \\ 0 & 0 & +1 & 0 \\ 0 & 0 & 0 & +1 \end{bmatrix}, \quad (3)$$

where the minus sign distinguishes time from space. Compute the change in components of a vector transported parallel to itself with the connection coefficients

$$\Gamma_{\mu\nu\sigma} = \frac{1}{2}(g_{\mu\nu,\sigma} + g_{\mu\sigma,\nu} - g_{\nu\sigma,\mu}), \quad (4)$$

where the commas denote differentiation with respect to the coordinate labeled by the following index. Raise and lower indices with the metric like

$$\Gamma_{\nu\sigma}^\mu = g^{\mu\lambda} \Gamma_{\lambda\nu\sigma}. \quad (5)$$

Calculate the change in a vector parallel transported around an infinitesimal parallelogram using the Riemann curvature tensor

$$R_{\nu\rho\sigma}^\beta = \Gamma_{\nu\sigma,\rho}^\beta - \Gamma_{\nu\rho,\sigma}^\beta + \Gamma_{\nu\sigma}^\alpha \Gamma_{\alpha\rho}^\beta - \Gamma_{\nu\rho}^\alpha \Gamma_{\alpha\sigma}^\beta. \quad (6)$$

Contract the Riemann tensor to get the Ricci tensor and scalar, $R_{\mu\nu} = R_{\mu\beta\nu}^\beta$ and $R = R_\mu^\mu$. Reverse the trace of the Ricci tensor to form the Einstein curvature tensor

$$G^{\mu\nu} = R^{\mu\nu} - \frac{1}{2} R g^{\mu\nu}. \quad (7)$$

2.2. Stress-energy

Record a particle's spacetime 4-momentum by

$$p^\mu \leftrightarrow \begin{bmatrix} p^0 \\ p^1 \\ p^2 \\ p^3 \end{bmatrix} = \begin{bmatrix} E \\ p^x \\ p^y \\ p^z \end{bmatrix}, \quad (8)$$

where $p^0 = E$ is energy and $\{p^x, p^y, p^z\}$ is spatial momentum. Relate the 4-momentum dp^μ to the 3-volume d^3V_v by

$$dp^\mu = T^{\mu\nu} d^3V_v, \quad (9)$$

where $T^{\mu\nu} = T^{\nu\mu}$ is the stress-energy tensor. Choose 3-volumes parallel to coordinate axes to write the stress-energy as 4-momentum per unit 3-volume with components

$$T^{\mu\nu} \leftrightarrow \frac{dp^\mu}{d^3V} \leftrightarrow \begin{bmatrix} \frac{dE}{dx dy dz} & \frac{dE}{dt dy dz} & \frac{dE}{dx dt dz} & \frac{dE}{dx dy dt} \\ \frac{dp^x}{dx dy dz} & \frac{dp^x}{dt dy dz} & \frac{dp^x}{dx dt dz} & \frac{dp^x}{dx dy dt} \\ \frac{dp^y}{dx dy dz} & \frac{dp^y}{dt dy dz} & \frac{dp^y}{dx dt dz} & \frac{dp^y}{dx dy dt} \\ \frac{dp^z}{dx dy dz} & \frac{dp^z}{dt dy dz} & \frac{dp^z}{dx dt dz} & \frac{dp^z}{dx dy dt} \end{bmatrix}. \quad (10)$$

In terms of forces F^k and areas A_i , the stress-energy components are

$$T^{\mu\nu} \leftrightarrow \begin{bmatrix} \frac{dE}{dV} & \frac{dE}{dt dA_x} & \frac{dE}{dt dA_y} & \frac{dE}{dt dA_z} \\ \frac{dp^x}{dV} & \frac{dp^x}{dA_x} & \frac{dp^x}{dA_y} & \frac{dp^x}{dA_z} \\ \frac{dp^y}{dV} & \frac{dp^y}{dA_x} & \frac{dp^y}{dA_y} & \frac{dp^y}{dA_z} \\ \frac{dp^z}{dV} & \frac{dp^z}{dA_x} & \frac{dp^z}{dA_y} & \frac{dp^z}{dA_z} \end{bmatrix}, \quad (11)$$

<i>t</i>	<i>x</i>	<i>y</i>	<i>z</i>
energy density	energy flux	energy flux	energy flux
mom density	pressure	shear	shear
mom density	shear	pressure	shear
mom density	shear	shear	pressure

Fig. 1. Symmetric stress-energy tensor $T^{\mu\nu}$ generalizes the stress tensor from space to spacetime.

which consolidates energy (and mass) density, energy fluxes, momentum densities, pressures, and shears in one geometrical object, as summarized by Fig. 1. Pressure T^{zz} stretches or compresses along the sole *z* direction, while shear pairs $T^{zx} = T^{xz}$ twist and anti-twist about the remaining *y* direction. Fig. 2 illustrates the pressures and shears in cylindrical coordinates for the cylindrical spaceship.

2.3. Field equations

Spacetime curvature is proportional to stress-energy

$$G^{\mu\nu} = 8\pi T^{\mu\nu}. \quad (12)$$

These are 10 nonlinear partial differential equations for the 10 unknown metric components $g_{\mu\nu}$. However, only 6 of the equations are independent, so they determine the metric only up to a general coordinate transformation. Invert this relation and write

$$T^{\mu\nu} = \frac{1}{8\pi} G^{\mu\nu} \quad (13)$$

to exploit the fact that differentiation is much easier than integration.

2.4. Geodesic equation

In curved spacetime, the law of inertia generalizes to the geodesic equation

$$\frac{d^2x^\mu}{d\tau^2} = -\Gamma_{\alpha\beta}^\mu \frac{dx^\alpha}{d\tau} \frac{dx^\beta}{d\tau}, \quad (14)$$

where, for massive particles, the affine parameter τ is the proper time, and the right side corrects for the turning and twisting of the basis vectors. A geodesic is the straightest possible path and also the path of extremal length (typically a minimum in space but a maximum in spacetime).

3. Artificial gravity field

Smoothly join curved spacetime inside a cylinder, representing the Earth gravity of the spaceship, with the flat spacetime outside the cylinder, representing interstellar space. Differentiate the spacetime metric to find the stress-energy in the cylinder's surfaces, which generates the artificial gravity field.

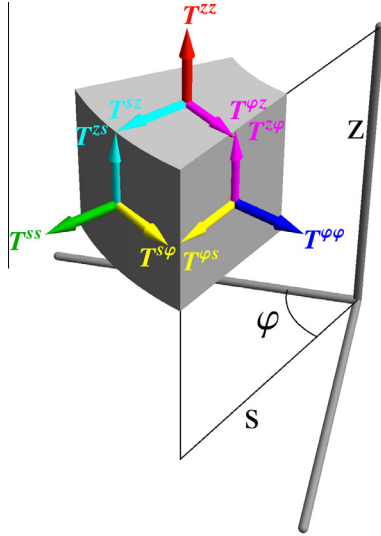


Fig. 2. Arrows suggest pressures T^{ii} (primary colors red, green, blue) and shears $T^i = T^{ji}$ (secondary colors yellow, magenta, cyan) on a cylindrical $\{s, \varphi, z\}$ volume element. Pressure pairs stretch or compress while shear pairs twist or counter twist.

3.1. Translated Schwarzschild metric

The spacetime outside a spherical mass m such as Earth is described by the Schwarzschild metric

$$g_{\mu\nu}^S \leftrightarrow \begin{bmatrix} -(1 - r_s/r) & 0 & 0 & 0 \\ 0 & (1 - r_s/r)^{-1} & 0 & 0 \\ 0 & 0 & r^2 & 0 \\ 0 & 0 & 0 & r^2 \sin^2 \theta \end{bmatrix}, \quad (15)$$

where t is faraway time, r is the reduced circumference, θ is colatitude, φ is longitude, and $r_s = 2m$ is the Schwarzschild radius. Following Moreau et al. [4], center the coordinates a translation Δ from the spherical mass by transforming the corresponding line element (including the differentials) to rectangular-like coordinates using

$$\begin{aligned} x &= r \sin \theta \cos \varphi, \\ y &= r \sin \theta \sin \varphi, \\ z &= r \cos \theta - \Delta. \end{aligned} \quad (16)$$

Next transform to cylindrical-like coordinates using

$$\begin{aligned} x &= s \cos \varphi, \\ y &= s \sin \varphi, \end{aligned} \quad (17)$$

where s is the perpendicular separation from the z -axis. The result [1] is the cylindrical-coordinates translated metric

$$g_{\mu\nu}^T \leftrightarrow \begin{bmatrix} r_s/\rho - 1 & 0 & 0 & 0 \\ 0 & \frac{\rho/r_s - (\Delta+z)^2/\rho^2}{\rho/r_s - 1} & 0 & \frac{s(\Delta+z)/\rho^2}{\rho/r_s - 1} \\ 0 & 0 & s^2 & 0 \\ 0 & \frac{s(\Delta+z)/\rho^2}{\rho/r_s - 1} & 0 & \frac{\rho(r_s - s^2)/\rho^2}{\rho/r_s - 1} \end{bmatrix}, \quad (18)$$

where $\rho = \sqrt{s^2 + (\Delta + z)^2}$. As a check, if the mass $m = r_s/2$ shrinks to zero, the translated metric reduces to the cylindrical-coordinates flat spacetime metric

$$g_{\mu\nu}^F = \lim_{m \rightarrow 0} g_{\mu\nu}^T \leftrightarrow \begin{bmatrix} -1 & 0 & 0 & 0 \\ 0 & 1 & 0 & 0 \\ 0 & 0 & s^2 & 0 \\ 0 & 0 & 0 & 1 \end{bmatrix}, \quad (19)$$

which implies the expected line element

$$d\sigma^2 = g_{\mu\nu}^F dx^\mu dx^\nu = -dt^2 + ds^2 + s^2 d\varphi^2 + dz^2. \quad (20)$$

3.2. Join

Because the Einstein field equations are second order partial differential equations, smoothly join the Eq. (18) translated Schwarzschild spacetime with the Eq. (19) flat spacetime using a C^2 unit box function. To begin the “surgery”, demand that a quintic function $f[\xi]$ pass through zero and unity, $f[0] = 0$ and $f[1] = 1$, and be doubly smooth at both ends, $f'[0] = f''[0] = 0$ and $f'[1] = f''[1] = 0$, to get

$$f[\xi] = 10\xi^3 - 15\xi^4 + 6\xi^5. \quad (21)$$

Use the quintic to form the one-dimensional unit box

$$\chi_1[\xi, \xi_0, w, \delta w] = \begin{cases} f\left[\frac{\xi - \xi_0 + w/2 + \delta w}{\delta w}\right] & : \xi_0 - w/2 - \delta w \leq \xi < \xi_0 - w/2 \\ 1 & : \xi_0 - w/2 \leq \xi < \xi_0 + w/2 \\ 1 - f\left[\frac{\xi - \xi_0 - w/2}{\delta w}\right] & : \xi_0 + w/2 \leq \xi < \xi_0 + w/2 + \delta w \\ 0 & : \text{else} \end{cases}, \quad (22)$$

where ξ_0 is the center, w is the width, and δw is the join thickness. From this, create a two-dimensional unit box

$$\chi_2[s, z] = \chi_1[s, \mathcal{R}/2, \mathcal{R}, \mathcal{T}] \chi_1[z, 0, \mathcal{H}, \mathcal{T}], \quad (23)$$

with radius \mathcal{R} , height \mathcal{H} , and thickness \mathcal{T} , as in Fig. 3. Describe all of spacetime by

$$g_{\mu\nu} = g_{\mu\nu}^F + \chi_2[s, z] (g_{\mu\nu}^T - g_{\mu\nu}^F). \quad (24)$$

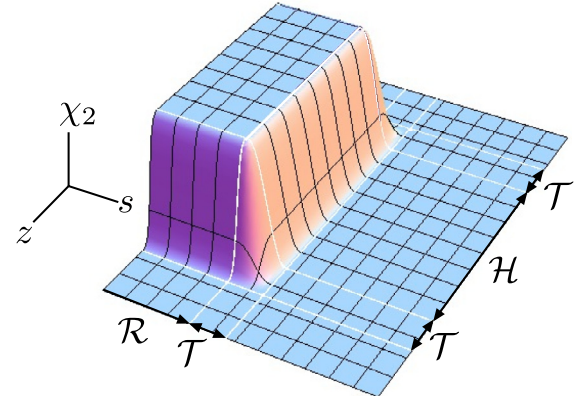
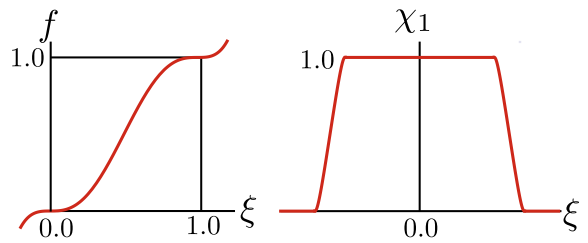


Fig. 3. Smooth function f creates one and two-dimensional unit box functions χ_1 and χ_2 to join flat and curved spacetime and localize the artificial gravity field.

At small distances $\chi_2 = 1$ and $g_{\mu\nu} = g_{\mu\nu}^T$, but at large distances, $\chi_2 = 0$ and $g_{\mu\nu} = g_{\mu\nu}^F$; inside the cylinder is curved Schwarzschild spacetime, but outside is flat Minkowski spacetime.

3.3. Stress-energy

Compute the stress-energy required to create this spacetime using the Eq. (13) field equations. This reduces to straightforward differentiation of the metric, which can be done by hand but is readily accomplished using computer algebra. The results are algebraic (albeit piecewise) solutions for the stress-energy. Although these expressions are complicated, they are nicely summarized in the Fig. 4 density plots. Each subplot is a vertical two-dimensional cross section of a normalized stress-energy component $T^{\hat{\mu}\hat{\nu}}$. (Appendix A describes the normalization and the supplement [1] contains vertical and radial one-dimensional cross sectional line plots.) Red is positive and blue is negative and magnitudes decrease with saturation, so white is zero. Parameters are mass $m = m_\oplus \approx 6.0 \times 10^{24}$ kg and translation $\Delta = R_\oplus \approx 6400$ km for Earth-like gravity, as well as a cylinder of height $H = 100$ m, radius $R = 50$ m, and thickness $T = 20$ m for the spaceship.

The stress-energy contains no energy flux or momentum density, as nothing moves in the spaceship's reference frame. There is no stress-energy in its cylindrical interior, which is good for our astronauts. However, there are nonzero energy densities, pressures, and shears in the wall, floor, and ceiling of its hull, where the flat and curved spacetimes join.

The ceiling includes a positive energy density layer of radial and azimuthal tension just under a layer of radial and azimuthal pres-

sure. The floor includes a negative energy density layer of radial and azimuthal pressure just under a layer of radial and azimuthal tension, the reverse of the ceiling. The wall includes a positive energy density thickness of vertical pressure just outside a negative energy density thickness of vertical tension, both under azimuthal twist and anti-twist. Peak energy densities are about 10^{26} J/m³ in the floor and ceiling and about 10^{31} J/m³ in the walls. Peak pressures are about 10^{31} Pa in the walls, while peak shears are only about 10^{25} Pa. Smaller stress-energies are too desaturated to be visible under the Fig. 4 palette.

The positive energy density in the ceiling and negative energy density in the floor are analogous to positive and negative charges creating a vertical electric field in a parallel plate capacitor. The horizontal bilayers of pressure and tension slow the interior proper time, as expected from the Schwarzschild metric. The vertical bilayer of pressure and tension coupled with the corresponding bilayer of positive and negative energy density increase the interior proper volume (by increasing the locally measured radial distances), again as expected. Nonuniform variations in the hull's stress-energy generate all the fine features of Earth-like gravity, including tidal effects. (Mathematically, the field equations differentiate the stepped metric twice to generate the bilayers.)

3.4. Other configurations

Repeating the calculations for a cubical spaceship necessitates a more complicated stress-energy distribution because of the vertical corners. Repeating for a spherical spaceship (to create a spacetime reminiscent of the Einstein–Straus vacuole metric [5,6] that joins a Schwarzschild and a Robertson–Walker metric) requires a more complicated stress-energy because the round hull encloses a “vertical” gravity field. Repeating for a weak-field approximation of the Schwarzschild metric inside a cylinder requires a simpler stress-energy distribution but unfortunately with horizontal pressure inside the spaceship (which is not surprising as the approximate metric is no longer an exact solution to the field equations). However, repeating for a Rindler uniform-gravity “flat Earth” metric [7] inside a cylinder requires comparable stresses confined to the hull with no net energy density (although negative energy density would need to cancel the positive energy density typically associated with the stresses). While the Rindler spacetime is algebraically simpler than the translated Schwarzschild spacetime, it does not exhibit tidal effects.

3.5. Testing

To test the artificial gravity field, numerically integrate the Eq. (14) geodesic equations for various initial conditions. A massive test particle released outside the spaceship does not move, but a mass released inside the spaceship falls with an Earth-like acceleration of $g_\oplus \approx 9.8$ m/s². Other tests [1] reveal tidal effects: while falling, pairs of particles released side-by-side slowly drift together, but pairs of particles released one-over-the-other drift apart. As expected, inside the cylinder horizontal light rays deflect downward but vertical light rays are undeflected.

Perhaps unexpectedly, the hull of the spaceship gravitationally confines slow moving particles. A mass released from rest bounces at the floor if its speed is less than a critical value. For Earth-like gravity, the critical speed is near the $v_\oplus \approx 11$ km/s Earth escape speed. Fast particles deflect as they pass through the floor but thereafter move in straight lines in flat Minkowski spacetime.

Fig. 5 illustrates typical geodesics for massive and massless test particles in an artificial gravity field scaled to nicely display the range of geodesics [1]. The bounces and deflections are completely gravitational, due to spacetime curvature. The confinement of slow particles inside the spaceship, where time runs slowly, is reminis-

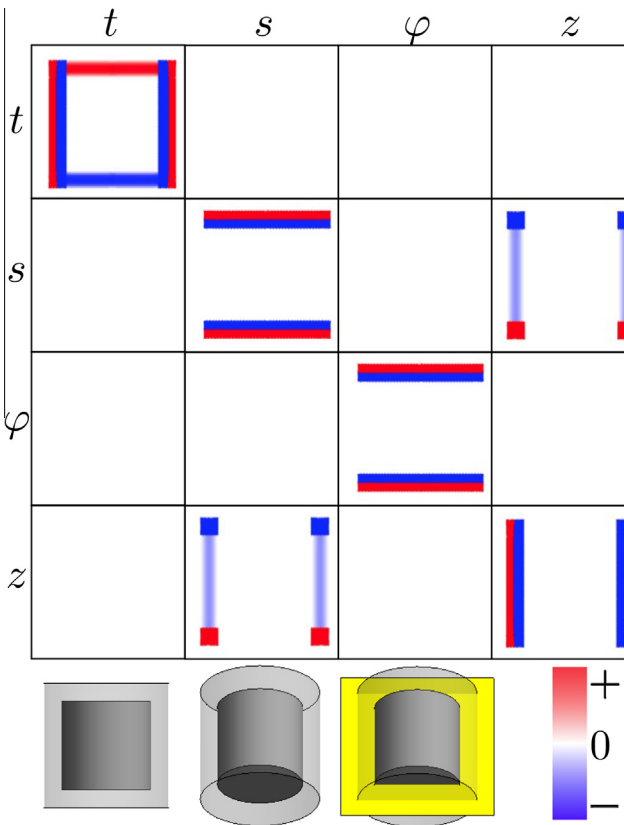


Fig. 4. Vertical cross sectional density plots (4×4 squares) illustrate the dominant contributions to the normalized stress-energy components $T^{\hat{\mu}\hat{\nu}}$ that warp spacetime to create an artificial gravity field (gray cylinder with yellow square marking the cross section). Red is positive and blue is negative and magnitudes decrease with saturation until they vanish at white.

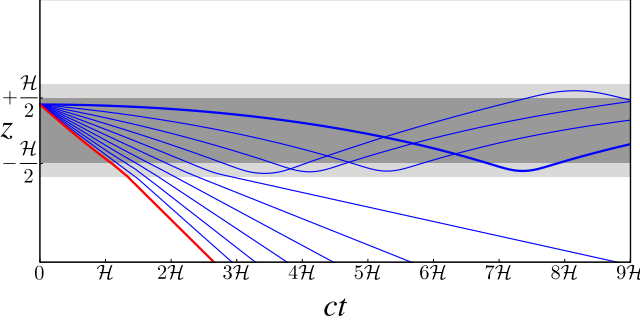


Fig. 5. Height z as a function of time ct . Inside a scaled artificial gravity field (dark gray between light gray floor and ceiling), a massive test particle falls as expected but bounces at the bottom (thick blue curve). Masses shot downward bounce if their bottom speeds are less than a critical speed but otherwise merely deflect (thin blue curves), as does a light ray (thick red curve).

cent of total internal reflection in an optical fiber. Indeed, under certain conditions, motion in curved spacetime can be described equivalently as motion in flat spacetime in a medium with a variable index of refraction [8,9].

3.6. Newtonian slab

To understand the importance of general relativity in designing an artificial gravity field, a Newtonian comparison is helpful. Consider a rectangular slab of thickness T , mass density ρ_M , and gravitational field g_\oplus just above its center. Imagine a short Gaussian cylinder of cross sectional area A vertically straddling the surface near its center. In analogy with Gauss's law for electricity, Gauss's law for Newtonian gravity

$$-g_\oplus 2A = \oint_{a=0, V} \vec{g}_\oplus \cdot d\vec{a} = \Phi_g = -4\pi GM_V = -4\pi G\rho_M AT \quad (25)$$

implies a mass density

$$\rho_M = \frac{g_\oplus}{2\pi GT} \sim 10^9 \frac{\text{kg}}{\text{m}^3} \quad (26)$$

and an energy density

$$T^{00} = \rho_M c^2 \sim 10^{26} \frac{\text{J}}{\text{m}^3}, \quad (27)$$

which is comparable to the floor and ceiling energy densities of the Fig. 4 artificial gravity field stress-energy tensor. Of course, at the corners of the slab the field is about 4 times smaller (as 4 identical slabs tiled at the corner would approximately restore the central field). Furthermore, the field below is opposite to that above!

3.7. Construction

Stretching, compressing, and twisting elastic material can, in principle, generate negative and positive pressures and shears to create the artificial gravity field. However, normal materials have strictly positive total energy density, and the artificial gravity field needs layers of positive *and* negative energy density. The necessary energy density decreases as the inverse square of the hull thickness T , which is consistent with the corresponding Newtonian density

$$\frac{U}{V} \sim \frac{GM^2/T}{AT} \propto \frac{1}{T^2}. \quad (28)$$

However, to make the spaceship well-defined, the thickness of the hull should be smaller than its radius, $T < R$.

Generating the negative energies is the hard part. For example, while a hydrogen atom does have a negative binding energy of -13.6 eV, this is overwhelmed by its positive mass-energy of about $+1$ GeV. Replace the electron by a more massive lepton like a muon

and the binding energy becomes more negative, but the total energy remains decisively positive.

If arbitrarily negative energy states existed, the vacuum would be unstable. In fact, various constraints on the stress-energy called weak and strong energy conditions are conjectured to hold for all "physically reasonable" matter [3]. If these conditions are violated, the matter is said to be "exotic". The Fig. 4 stress-energy violates these energy conditions and so is exotic. However, other recently studied spacetimes including the Alcubierre warp-drive [10,11] and the Morris-Thorne wormhole [12,13] appeal to violations of the weak energy condition and rely on negative energy density.

Quantum field theory provides possible sources of negative energy density. In squeezed vacuum states, destructive quantum interference can suppress vacuum fluctuations, so that locally the vacuum has less energy than it normally does. In one interpretation of the Casimir effect, nearby conductors suppress vacuum fluctuations between them producing negative energy density and a force that has been precisely measured [14,15]. The Hawking evaporation of a black hole can be understood as negative energy density flowing into its event horizon to balance the positive-energy radiation escaping to infinity. However, quantum inequalities suggest that assembling *macroscopic* quantities of negative energy density may be challenging or impossible [16].

4. Conclusions

Using computer algebra to run Einstein's equations "backward" is an illuminating tool to further our understanding of general relativity [17–20]. We are learning how pressures, tensions, and shears – as well as energy – can modify spacetime in simple examples, as part of a larger project to better understand the relationship between spacetime curvature and stress, energy, and momentum. We designed an artificial gravity field for a spaceship, but using simple stress-energy distributions one can readily design "closets" that are larger on the inside than on the outside or "refrigerators" where time runs slowly (to keep food fresh). Although the engineering [11] of these spacetimes seems daunting or impractical, experimentalists may be able to exploit quantum phenomena like squeezed vacuum states and the Casimir effect to perturb spacetime in microscopic regions and probe the perturbations with sensitive interferometers.

Even if such exotic spacetimes are ultimately unphysical, they are exact solutions to Einstein's equations. They excite the imagination and help us better grasp the structure of general relativity, which nearly a hundred years after its introduction remains our best confirmed theory of gravity.

Acknowledgment

We thank Brian Maddock for asking the question.

Appendix A. Normalizing the stress-energy

In general relativity, it is common to calculate in an unnormalized coordinate basis, but interpret the results in an orthonormal basis [2]. Normalization is more complicated if the metric is non-diagonal, as is the case for both the astrophysically important Kerr spacetime of a rotating black hole and the Eq. (24) artificial gravity spacetime.

The scalar products of the unnormalized basis vectors $\mathbf{e}_\mu = \partial \mathbf{r} / \partial x^\mu$ are the general metric components

$$\mathbf{e}_\mu \cdot \mathbf{e}_\nu = g_{\mu\nu}, \quad (\text{A.1})$$

while the scalar products of the normalized basis vectors \mathbf{e}_μ are the Minkowski metric components

$$\mathbf{e}_{\hat{\mu}} \cdot \mathbf{e}_{\hat{\nu}} = \eta_{\mu\nu}.$$

Expand a rank-one tensor (or vector) as

$$\mathbf{v} = v^\mu \mathbf{e}_\mu = v^{\hat{\nu}} \mathbf{e}_{\hat{\nu}}, \quad (\text{A.3})$$

and expand a rank-two tensor as

$$\mathbf{t} = t^{\mu\nu} \mathbf{e}_\mu \otimes \mathbf{e}_\nu = t^{\hat{\alpha}\hat{\beta}} \mathbf{e}_{\hat{\alpha}} \otimes \mathbf{e}_{\hat{\beta}}, \quad (\text{A.4})$$

where the tensor product \otimes is the most general bilinear product.

For a metric of the form

$$g_{\mu\nu} \leftrightarrow \begin{bmatrix} g_{tt} & 0 & 0 & 0 \\ 0 & g_{ss} & 0 & g_{sz} \\ 0 & 0 & g_{\varphi\varphi} & 0 \\ 0 & g_{sz} & 0 & g_{zz} \end{bmatrix}, \quad (\text{A.5})$$

the vectors

$$\begin{aligned} \mathbf{e}_t &= \frac{1}{\sqrt{-g_{tt}}} \mathbf{e}_t, \\ \mathbf{e}_s &= \frac{g_{zz} \mathbf{e}_s - g_{sz} \mathbf{e}_z}{\sqrt{g_{zz}} \sqrt{g_{ss} g_{zz} - g_{sz}^2}}, \\ \mathbf{e}_\varphi &= \frac{1}{\sqrt{g_{\varphi\varphi}}} \mathbf{e}_\varphi, \\ \mathbf{e}_z &= \frac{1}{\sqrt{g_{zz}}} \mathbf{e}_z, \end{aligned} \quad (\text{A.6})$$

are orthonormal, as is readily verified [1]. The orthonormal components of a rank-one tensor are the projections

$$\mathbf{v}_{\hat{\alpha}} = \mathbf{e}_{\hat{\alpha}} \cdot \mathbf{v} = (\mathbf{e}_{\hat{\alpha}})^\mu v_\mu, \quad (\text{A.7})$$

where the coordinate basis components of the orthonormal basis vectors $(\mathbf{e}_{\hat{\alpha}})^\mu$ are easily identified from Eq. (A.6). Similarly, the orthonormal components of a rank-two tensor are

$$t_{\hat{\alpha}\hat{\gamma}} = (\mathbf{e}_{\hat{\alpha}})^\mu (\mathbf{e}_{\hat{\gamma}})^\nu t_{\mu\nu}, \quad (\text{A.8})$$

and this suffices to normalize the stress-energy.

(A.2)

Appendix B. Supplementary data

Supplementary data associated with this article can be found, in the online version, at <http://dx.doi.org/10.1016/j.rinp.2013.01.003>.

References

- [1] See supplementary material in Appendix B for a *Mathematica* notebook (in PDF format) that provides the algebra and numerics for all the results in this paper.
- [2] Hartle JB. Gravity: An introduction to Einstein's general relativity. Addison Wesley; 2003.
- [3] d'Inverno R. Introducing Einstein's relativity. Oxford University Press; 2000.
- [4] Moreau W, Neutze R, Ross DK. The equivalence principle in the Schwarzschild geometry. *Am J Phys* 1994;62:1037–40.
- [5] Einstein A, Straus EG. The influence of the expansion of space on the gravitation fields surrounding the individual stars. *Rev Mod Phys* 1945;17:120–4.
- [6] Einstein A, Straus EG. Corrections and additional remarks to our paper: the influence of the expansion of space on the gravitation fields surrounding the individual stars. *Rev Mod Phys* 1946;18:148–9.
- [7] Rindler W. Relativity: special, general and cosmological. 2nd. Oxford University Press; 2006.
- [8] Eddington AS. Space, time and gravitation. Cambridge University Press; 1920.
- [9] Evans J, Nandi KK, Islam A. The optical-mechanical analogy in general relativity: exact Newtonian forms for the equations of motion of particles and photons. *Gen Rel Grav* 1996;28:413–39.
- [10] Alcubierre M. The warp-drive: hyper-fast travel within general relativity classical. *Quant Grav* 1994;11:L73–7.
- [11] White H. A Discussion on space-time metric engineering. *Gen Rel Grav* 2003;35:2025–33.
- [12] Morris MS, Thorne KS, Yurtsever U. Wormholes, times machines, and the weak energy condition. *Phys Rev Lett* 1988;61:1446–9.
- [13] Morris MS, Thorne KS. Wormholes in spacetime and their use for interstellar travel: a tool for teaching general relativity. *Am J Phys* 1988;56:395–412.
- [14] Casimir HBG. On the attraction between two perfectly conducting plates. *Proc K Ned Akad Wet* 1948;51:793–6.
- [15] Mohideen U, Roy. Precision measurement of the Casimir force from 0.1 to 0.9 μm. *Phys Rev Lett* 1998;81:4549–52.
- [16] Ford LH, Roman TA. The quantum interest conjecture. *Phys Rev D* 1999;60:104018.
- [17] Jonsson RM. Visualizing curved spacetime. *Am J Phys* 2005;73:248–60.
- [18] Tredafilova CS, Fulling SA. Static solutions of Einstein's equations with cylindrical symmetry. *Eur J Phys* 2011;32:1663–77.
- [19] Müller T, Frauendiener J. Interactive visualization of a thin disc around a Schwarzschild black hole. *Eur J Phys* 2012;33:955–63.
- [20] Jones P, Muñoz G, Ragsdale M, Singleton D. The general relativistic infinite plane. *Am J Phys* 2008;76:73–8.